General Disclaimer

One or more of the Following Statements may affect this Document

- This document has been reproduced from the best copy furnished by the organizational source. It is being released in the interest of making available as much information as possible.

- This document may contain data, which exceeds the sheet parameters. It was furnished in this condition by the organizational source and is the best copy available.

- This document may contain tone-on-tone or color graphs, charts and/or pictures, which have been reproduced in black and white.

- This document is paginated as submitted by the original source.

- Portions of this document are not fully legible due to the historical nature of some of the material. However, it is the best reproduction available from the original submission.

CR-151924

Princeton University

Department of Aerospace and Mechanical Sciences

(NASA-CR-151924) AN EXPERIMENTAL INVESTIGATION OF THE FLAP-LAG STABILITY OF A HINGELESS ROTOR WITH COMPARABLE LEVELS OF HUB AND BLADE STIFFNESS IN HOVERING FLIGHT Final Report (Princeton Univ., N.J.) 33 p G3/05

N77-12040
HC A03
MF A01
Unclas
56723

CR-151924

AN EXPERIMENTAL INVESTIGATION OF THE FLAP-LAG STABILITY OF A HINGELESS ROTOR WITH COMPARABLE LEVELS OF HUB AND BLADE STIFFNESS IN HOVERING FLIGHT

by

H. C. Curtiss, Jr.
W. F. Putman

AMS Report No. 1300

June 1976

FINAL REPORT

PREPARED UNDER

NASA-Ames Research Center
Ames Directorate
U. S. Army Air Mobility R&D Laboratory
Moffett Field, California

Contract Number NAS 2-7615

Princeton University
Department of Aerospace and Mechanical Sciences

FOREWORD

This final report was prepared by the Department of Aerospace and Mechanical Sciences, Princeton University, Princeton, New Jersey under Contract Number NAS 2-7615 with NASA-Ames Research Center. It was funded by and under the technical direction of the U. S. Army Air Mobility Research and Development Laboratory, Ames Directorate, Ames Research Center at Moffett Field, California and was monitored and administered by Dr. Dewey Hodges of that directorate.

Mr. William G. Bousman of the Ames Directorate, provided valuable assistance during the set up of the experiments and by performing the theoretical calculations used in comparing the experimental results with theory.

SUMMARY

The results of an experimental investigation of the flap-lag stability of a hingeless rotor in hovering flight are presented and discussed. The rotor blade and hub configuration were selected such that the hub and blade had comparable levels of bending stiffness.

The experimental results presented here complement experimental results reported in the literature. In these previous experiments all of the bending flexibility in the rotor system was provided by the hub and the blade was effectively rigid.

TABLE OF CONTENTS

LIST OF FIGURES

NOMENCLATURE

a	blade section lift curve slope
c	blade chord, in or ft
I	blade moment of inertia in flap direction with respect to flap flexure ($r = 1.25$ in), slug-ft^2
I_{cg}	blade moment of inertia in flap direction with respect to blade center of gravity, lb-in^2
K	Southwell coefficient
r	local radius, measured from axis of rotation, in
R	rotor radius, in, or elastic coupling parameter defined in References 1 and 2
R_E	Reynolds number at three-quarters radius, $R_E = \frac{.75\,\Omega Rc}{\nu}$
W_B	blade weight, lbs
W_s	blade weight moment with respect to flap flexure ($r = 1.25$ in), lb-in
γ	Lock number, $\frac{\rho acR^4}{I}$
η_m	structural damping ratio of lag motion
θ	blade pitch angle at three-quarters radius
θ_s	structural pitch angle, $\theta_s = \theta_{so} + \theta$
θ_{so}	structural pitch angle at $\theta = 0$, inclination of principal flexural axes of blade-hub system measured with respect to blade chord line at three-quarters radius

ν	kinematic viscosity of air, ft^2/sec
ρ	air density, $slugs/ft^3$
ω_β	uncoupled non-rotating rotor blade natural frequency in flap ($\theta_s = 0$) Hz
ω_{β_B}	non-rotating blade natural frequency in flap direction, rigidly mounted, Hz
ω_ζ	uncoupled non-rotating rotor blade natural frequency in lag ($\theta_s = 0$), Hz
ω_{ζ_B}	non-rotating blade natural frequency in lag direction, rigidly mounted, Hz
ω_1 , ω_2	non-rotating natural frequencies of rotor blade at pitch angles other than $\theta_s = 0$, Hz
Ω	rotor angular velocity, RPM
$\bar{(\ )}$	frequency non-dimensionalized by rotor RPM
$(\ )_C$	value of quantity in chordwise or lag direction
$(\ )_F$	value of quantity in flapwise direction

INTRODUCTION

This report describes the results of an experimental investigation of the flap-lag stability of a hingeless helicopter rotor blade and compares the experimental results with theory. The theory used for comparison is presented in References 1 and 2.

It has been shown in Reference 1 that the distribution of elastic stiffness between the rotor hub and the rotor blade has a significant influence on the dynamics of the coupled flap-lag motion of a hingeless rotor blade and consequently affects the damping of the lag motion. The relative distribution of stiffness between the hub and the blade can be characterized by an elastic coupling parameter, denoted by R in References 1 and 2. The parameter R is defined, such that, values of zero and one represent limits of the ratio of blade stiffness to hub stiffness. A value of R equal to zero represents a blade-hub configuration in which the hub is flexible and the blade is rigid. R equal to one characterizes the case in which the blade is flexible and the hub is rigid. An alternate physical interpretation of the parameter R is associated with the rotation of the principal flexural axes of the blade-hub system with blade pitch. When R is equal to zero, the blade principal axes remain aligned with the shaft as the pitch is varied, and when R is equal to one the principal axes rotate in a one-to-one relationship with the blade pitch.

Experimental results are presented in Reference 2 for two values of the elastic coupling parameter R near to each of these limits ($R = 0.08$ and $R = 0.96$). It was the object of the experiments

described here to obtain data for an intermediate value of R, nominally 0.5, and to compare these results with the theory of References 1 and 2.

The experimental apparatus employed in these experiments consisted of the drive system and rotor hub described in Reference 2. Rotor blades fabricated at Princeton and described in detail later in this report were employed to obtain a value of the elastic coupling parameter nominally equal to 0.5.

This report is the final report submitted under NASA-Ames Research Center Contract Number NAS 2-7615 and comprises one of a number of investigations conducted under the subject contract. References 3, 4, 5, and 6 describe other investigations conducted at Princeton University related to flap-lag stability which were submitted under this contract. Reference 3 is a theoretical study concerned with the sensitivity of analytical predictions of flap-lag stability to various modelling assumptions. References 4, 5, and 6 are concerned with fundamental aspects of modelling flexible rotor blades undergoing large structural deformations.

EXPERIMENTAL APPARATUS

Thrust Stand

The model rotor thrust stand and hub employed for these experiments was loaned to Princeton University by the Ames Directorate of AMRDL. The shaker described in Reference 2 was not supplied, so an electromechanical shaker was designed and constructed at Princeton University to provide suitable excitation of rotor blade lag motion. The thrust stand is shown in the photograph in Figure 1 with the electromechanical shaker installed.

Rotor Hub

The rotor hub used is described in detail in Reference 2 and shown in Figure 2. Hub Stiffness is simulated by two sets of flexures, one providing flap flexibility and the other providing lag flexibility. The flexures were placed as close as possible to the axis of rotation to minimize the effects of hinge offset. The flexures were designed to provide high torsional rigidity. The blade pitch angle can either be varied inboard, close to the axis of rotation, or outboard at the blade root. In fact, in the experiments reported in Reference 2, the two limiting values of the elastic coupling parameter R were obtained by varying the pitch at these two locations to simulate the two different values of R. As noted in the Introduction, R can be directly associated with the rotation of the blade-hub system principal flexural axes with blade pitch angle[7]. The rotor blades employed in the experiments of Reference 2 were very stiff. The value of R near one was obtained by changing the pitch at the inboard location such that the hub flexures rotate with the blade when the pitch angle is changed. The value of R

near zero, corresponding to v y little rotation of the principal flexural axes with blade pitch, was obtained by changing blade pitch at the outboard location, such that, the hub flexures remain at a fixed orientation with respect to the rotor shaft.

For experiments reported here, flexible rotor blades were used with this hub to obtain an intermediate value of R. The blade pitch was changed by adjustments at the outboard pitch change location only. The inboard flap flexure axis was perpendicular to the rotor shaft. The blade flexibility combined with the hub flexibility gave a nominal value of R = 0.5.

Rotor Blades

The rotor blades were constructed of expanded light weight foam plastic with a Fiberglass skin. A leading edge spar places the elastic axis and the sectional center of gravity of the blade at the one-quarter chord location. The rotor blades were fabricated in a mold using the foam plastic to provide the basic aerodynamic shape of the blade and the Fiberglass skin to provide a smooth surface and appropriate bending stiffness.

The rotor blade airfoil section is a NACA 0015, and the blade is linearly twisted. Table I lists the blade and rotor characteristics. The local inertial and stiffness properties of the blades are presented in Figure 3. The non-rotating natural frequencies listed in Table I were determined experimentally. The torsional frequency is very high and it is therefore assumed in the analysis that the blade is rigid in torsion. Figure 4 gives the pertinent dimensions of the blade-hub system, and indicates by cross-hatching the part referred to as the blade.

Instrumentation

Strain gages mounted on the hub flexures were employed to measure

the blade motion. It was determined during the course of the experiments that there was an extraneous frequency of approximately 25 Hz appearing in the lag strain gage readings which made it difficult to measure the damping of the lag mode. This frequency is apparently a natural frequency of the thrust stand, and it appeared with equal amplitude and phase in the lag reading of each blade and was removed from the data by reading the difference between the lag bending signal of each blade. This technique eliminated the presence of this unwanted frequency and made it possible to obtain good measurements of the damping of the lag motion. There was also an excitation of the lag motion near one per rev present at various rotational speeds. The source of this disturbance was not discovered during the course of the experiments and presented some difficulty in the determination of lag damping at the higher rotor rotational speeds (above 300 RPM). However, it was possible to obtain good values of the lag damping over the rotational speed range of interest in these experiments.

Experimental Procedure

The electromechanical shaker was used to provide a horizontal sinusoidal motion of the rotor hub which in turn excited the lag motion of the rotor blades. The rotor was adjusted to a particular RPM of interest and then the shaker tuned to provide a maximum response. Then after the lag motion was excited, the shaker was turned off and the lag motion allowed to naturally decay. The damping ratio was measured from the decay rate of the lag trace. Averages were taken over a large number of cycles to determine the best value of the lag damping as a function of blade pitch and rotational speed.

TABLE I

ROTOR AND BLADE CHARACTERISTICS

Blade*

Weight, W_B	1.16 lb.
Flapping moment of inertia about blade center of gravity, I_{CG}	244 lb-in^2
Natural frequencies (rigidly mounted), non-rotating	
Flapwise, ω_{β_B}	4.09 Hz
Chordwise, ω_{ζ_B}	16.3 Hz
Torsion, ω_{θ_B}	98.4 Hz

Rotor

Radius, R	51.75 in
Chord, c	2.50 in
Number of blades, b	2
Airfoil Section	NACA 0015
Twist, θ_1	-.167°/in
Spanwise center of gravity, r_{CG}	18.85 in
Moment of inertia about the root of flap flexure, (r = 1.25 in.), I	602 lb-in^2
Weight moment about the root of flap flexure, (r = 1.25 in.), W_s	20.34 lb-in
Lock number	7.74
Structural pitch angle, θ_{so}	4°
Structural damping in lag	.003
Uncoupled natural frequencies (blade pitch angle = - θ_{so}), non-rotating	
ω_β	2.70 Hz
ω_ζ	6.28 Hz
ω_θ	95.6 Hz

*See Figure 4 for definition of blade and hub.

DISCUSSION

Experimental measurements of the lag damping were made for various values of rotor rotational speed and blade pitch angle. Specifically at a blade pitch angle of 8° at three-quarters radius, the lag damping was determined over a range of rotational speeds from 200 RPM to 320 RPM and also over a range of blade pitch angles from 0° to 8°.

The dimensionless rotating natural frequencies of the rotor blade-hub system at zero structural pitch angle are shown in Figure 5. These rotating frequencies are calculated based on experimental measurement of the non-rotating frequencies and the simplifying assumption that the Southwell coefficient is equal to one for flap bending and equal to zero for lag bending. Consequently the lag natural frequency is independent of rotor rotational speed. It can be seen from this figure that the rotor under investigation is stiff-in-plane ($\bar{\omega}_{\zeta} > 1$). The structural damping of the lag motion for the blade-hub system was experimentally determined to be 0.3 percent of critical.

In order to compare the experimental results with the theory of Reference 1 and 2, a number of other measurements are necessary. The theory presented in References 1 and 2 is based on a simplified physical model of the elastic characteristics of the blade-hub system. This simplified model represents the hub as massless with its flexibility modelled by a pair of orthogonal springs which remain at a fixed orientation with respect to the shaft. The blade flexibility is modelled by a second pair of orthogonal springs which rotate with blade pitch. With this physical model it is shown[1,2] that the dynamic characteristics of

the rotor-hub system can be characterized by four parameters in addition to the blade pitch angle. These four parameters are: the elastic coupling parameter R; the structural pitch angle θ_s, which is the inclination of the blade principal flexural axes at zero blade pitch angle; and the non-rotating flap and lag frequencies of the blade-hub system. The elastic coupling parameter R is calculated from various experimental data obtained on the non-rotating blade-hub system. Three essentially different techniques, described in detail in Reference 7, are available for the determination of R.

The most direct approach is through measurement of the rotation of the principal axis of the blade-hub system with blade pitch angle. It can be shown[3] that the rotation of the principal axes with blade structural pitch angle is related to the parameter R by the equation

$$\tan 2\gamma_p = \frac{R \sin 2\theta_s}{R \cos 2\theta_s + (1 - R)} \tag{1}$$

This approach has the advantage that no frequency measurements are required. Further, good values of R can be obtained at small values of θ_s, typical of the operating condition of a helicopter rotor[7].

A second method is directly suggested by the results of Reference 2 and is, in fact, the method employed in that Reference. It can be shown that the non-rotating natural frequencies of the blade-hub system vary with pitch angle and R as a function of the non-rotating frequencies at zero structural pitch angle (ω_β, ω_ζ) in the following fashion

$$\omega_{1,2} = \left[\frac{2\,\omega_\beta^2\,\omega_\zeta^2}{(\omega_\zeta^2 + \omega_\beta^2) \pm (\omega_\zeta^2 - \omega_\beta^2)\sqrt{1 - 4\,(1 - R)\,R \sin^2 \theta_s}} \right]^{\frac{1}{2}} \tag{2}$$

Thus, the natural frequencies can be measured at a variety of blade pitch angles, and with the values of the frequencies at zero structural pitch angle (ω_β, ω_ζ), R can be calculated. Using this technique, large variations in blade pitch angle are required, since for small pitch angles the frequencies vary with the square of the pitch angle and consequently, the value of R obtained is very sensitive to the experimental measurement of the frequencies. The sensitivity of this approach at small pitch angles is shown by the fact that for this particular rotor configuration at a structural pitch angle setting of 34°, a three percent variation in flap frequency from the value at zero pitch angle results in variation of R from 0 to 0.5. Consequently, a large pitch angle range is required. For this reason, measurements of the natural frequencies were made at 0°, 30°, 60° and 90° pitch, rather than over the normal operating range of the rotor. Also it should be noted that equation (2) is quadratic in R and therefore two values of R result from the use of equation (2). An additional relationship is required to determine the proper value of R. Equation (1) gives the additional relationship, since the inclination of the axes along which the two oscillations take place is equal to the inclination of the principal flexural axes of the blade-hub system. If these directions are measured, the proper value of R can be determined from equation (1). Here, an approximate measurement is satisfactory to distinquish whether the proper value of R is greater or less than 0.5, since the frequency measurements are used to determine the quantitative value of R.

A third approach is also possible using a somewhat different set of data. The measured non-rotating natural frequencies of the rotor blade

with the rotor blade root rigidly mounted, rather than on the hub, can be used with the measured non-rotating natural frequencies of the blade mounted on the hub to determine the elastic coupling parameter R.

Denoting by ω_{ζ_B} and ω_{β_B} the natural frequencies of the rotor blade with the root rigidly mounted, it may be shown from the definition of R given in Reference 2 and the results of Reference 3 that R is given by

$$R = \left(\frac{1 - \left(\frac{\omega_{\beta_B}}{\omega_{\zeta_B}}\right)^2}{1 - \left(\frac{\omega_\beta}{\omega_\zeta}\right)^2} \right) \left(\frac{\omega_\beta^2}{\omega_{\beta_B}^2} \right) \tag{3}$$

where ω_β and ω_ζ are the natural frequencies of the blade-hub system. This technique was also used to calculate R as described below.

Data are presented in Figure 6 for the natural frequencies at various pitch angles and the orientation of the two oscillations at a pitch angle of 90°. These results taken with the measured structural pitch angle $\theta_{so} = 4^\circ$, are used with equations (1) and (2) to determine the values of R given in Figure 7. Also shown in Figure 7, is the value of R determined by the technique expressed by equation (3). Table I gives the experimental values of the non-rotating natural frequencies of the blade with a rigid root mounting. There is some variation in R with pitch angle, apparently a result of the approximations used to develop the parameter R. The value of R determined from the flap mode is not shown at 30° due to the sensitivity of the calculation as noted above. Calculation of R based on the frequency

which is predominately motion in the lag direction gives a value of R which is less sensitive to the precise value of the frequency than use of the frequency in the flap direction.

The physical explanation for the variation of the calculated value of R indicated in Figure 7 is not apparent, however, it is undoubtedly related to approximations contained in the mathematical model which represents the rotor as a lumped parameter system where in actual fact the blade employed in these experiments is characterized by distributed flexibility and mass.

Comparison of Theory and Experiment

The experimental measurements of the damping ratio of the lag mode as a function of blade pitch and rotor angular velocity are presented in Figures 8 through 10. Figures 8 and 9 show the variation of lag damping with blade pitch angle at 200 RPM and 300 RPM respectively. Figure 10 shows the experimental variation of lag damping with rotor RPM at a blade pitch angle of 8°.

The theoretical results presented include two different analytical descriptions of the rotor blade section aerodynamic characteristics, referred to as linear theory and non-linear theory. For the linear theory, the blade section lift curve slope and the profile drag coefficient are assumed to be constant. The lift curve slope used in the linear theory is 5.73. Two values of the blade profile drag coefficient were used. At 200 RPM, the Reynolds number at three-quarters radius is 88,100. The experimental data presented in Reference 8, for a NACA 0015 airfoil, indicate that at this Reynolds number, a profile drag

coefficient of .02 at zero lift should be used for correlation with theory. The Reynolds number at three quarters radius is 132,100 at 300 RPM. Reference 8 indicates that the blade profile drag coefficient has decreased to approximately .01 at zero lift. The non-linear theory incorporates dependence of the lift coefficient and the profile drag coefficient on angle-of-attack representative of the blade airfoil section at the Reynolds number of these experiments. A detailed description of the airfoil characteristics employed in the non-linear theory may be found in Reference 2. The analytical model of the airfoil data employed is characteristic of the NACA 0012 section at a $R_E \cong 1.5 \times 10^6$. The behavior of the NACA 0015 section at this Reynolds number is similar to the NACA 0012.

The physical parameters of the rotor are given in Table I, and a tip loss of .97 was used.

The value of R used for the comparison was chosen to be 0.5 based on the results of the third technique described above. As can be noted from Figure 6, determination of R at larger pitch angles gave values smaller than 0.5. However, since the experiments were concerned with blade pitch angles smaller than 10°, it would be expected that the best choice for the value of R is that determined at zero pitch angle. Figure 11 indicates the effect of R on lag mode damping, showing the comparison of the predicted lag mode damping for R = 0.4 and R = 0.5. R = 0.4 is the value of the elastic coupling parameter determined from experiments at 90° pitch angle. It appears from Figure 11, that the possible

variation in R indicated by Figure 7 over the pitch angle range of these experiments, is not significant.

The linear theory agrees quite well with the experimental results using a value of R = 0.5 as can be seen from Figures 8, 9 and 10. The non-linear theory yields somewhat higher values of lag damping at the higher pitch angles. Non-linear theory is not shown at 200 RPM owing to the low Reynolds number for this case. Agreement with the linear theory is very good at 200 RPM. At 300 RPM the trend also appears to be predicted well with the exception of the experimental point at a blade pitch angle of about 5.8°. The experimental point at a blade pitch angle of 8° falls between the linear and non-linear calculations. The variation of lag damping ratio with RPM also is predicted very satisfactorily by the theory as shown in Figure 10. The results at higher RPM fall between the linear and non-linear theory. It would appear from the theoretical curves that the increase in the lag damping ratio at 200 RPM indicated by the experimental results is a Reynolds number effect as indicated by the theoretical curves for two values of the blade profile drag coefficient.

It therefore generally appears that the theory of References 1 and 2 is quite successful at predicting the lag damping for a rotor system with comparable levels of blade and hub stiffness.

The theoretical calculations were performed by Mr. W. G. Bousman of the Ames Directorate of the U. S. Army Air Mobility R&D Laboratory.

CONCLUSIONS

On the basis of the experiments conducted, the following conclusions may be drawn:

1.) The theory for flap-lag stability of hingeless rotor blades presented in References 1 and 2 is quite successful in predicting the damping of the lag mode of a rotor system with comparable levels of hub and blade stiffness.

2.) A single elastic coupling parameter, R developed in References 1 and 2 appears to be inadequate to describe the elastic characteristics of a rotor blade hub system over the pitch angle range from 0 to 90°, however, it appears quite satisfactory for a description of the system over the range of pitch angles normally encountered in helicopter flight.

REFERENCES

1. Ormiston, R. A. and Hodges, D. H.: "Linear Flap-Lag Dynamics of a Hingeless Helicopter Rotor Blade in Hover", Journal of the American Helicopter Society, Vol. 17, No. 2, April 1972.

2. Ormiston, R. A. and Bousman, W. G.: "A Study of Stall-Induced Flap-Lag Instability of Hingeless Rotors", Journal of the American Helicopter Society, Vol. 20, No. 1, January 1975.

3. Curtiss, H. C., Jr.: "Sensitivity of Hingeless Rotor Blade Flap-Lag Stability in Hover to Analytical Modelling Assumptions", Princeton University Aerospace and Mechanical Sciences Technical Report No. 1236, January 1975.

4. Dowell, E. H.: "A Variational-Rayleigh-Ritz Modal Approach For Non-Uniform Twisted Rotor Blades Undergoing Large Bending and Torsional Motion", Princeton University Aerospace and Mechanical Sciences Technical Report No. 1193, November 1974.

5. Dowell, E. H. and Traybar, J. J.: "An Experimental Study of the Non-linear Stiffness of a Rotor Blade Undergoing Flap, Lag and Twist Deformations", Princeton University Aerospace and Mechanical Sciences Technical Report No. 1194, January 1975.

6. Dowell, E. H. and Traybar, J. J.: "An Experimental Study of the Non-linear Stiffness of a Rotor Blade Undergoing Flap, Lag and Twist Deformations", Princeton University Aerospace and Mechanical Sciences Technical Report No. 1257, December 1975.

7. Suermann, T. C.: "An Experimental Investigation of Structural Characteristics of Hingeless Helicopter Rotors With Respect to Flap-Lag Stability", Princeton University Aerospace and Mechanical Sciences M.S.E. Thesis No. T-1221, May 1975.

8. Jacobs, E. N. and Sherman, A.: "Airfoil Section Characteristics as Affected by Variations of the Reynolds Number", NACA Report No. 586, June 1936.

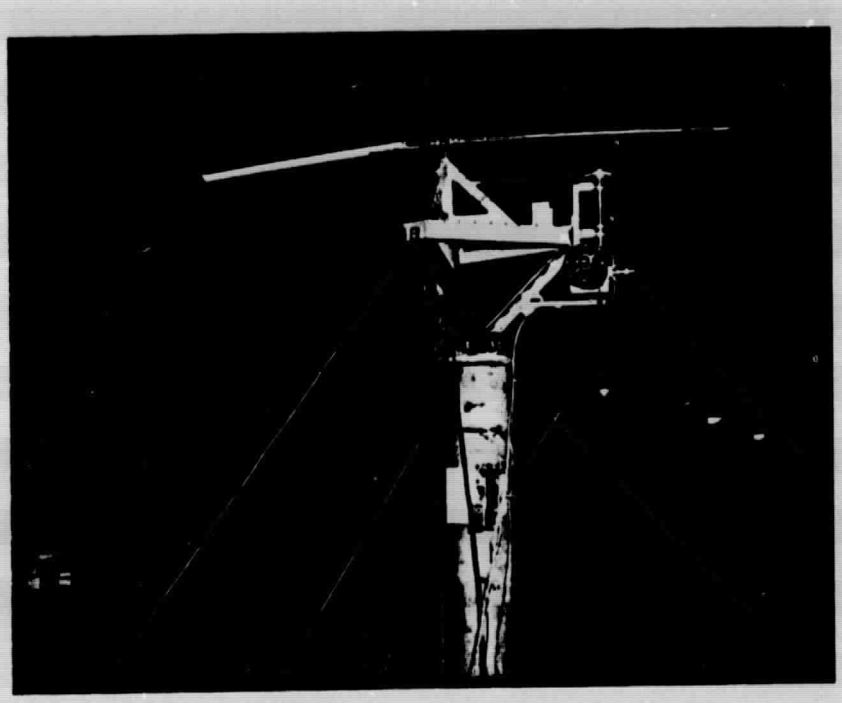

Overall View

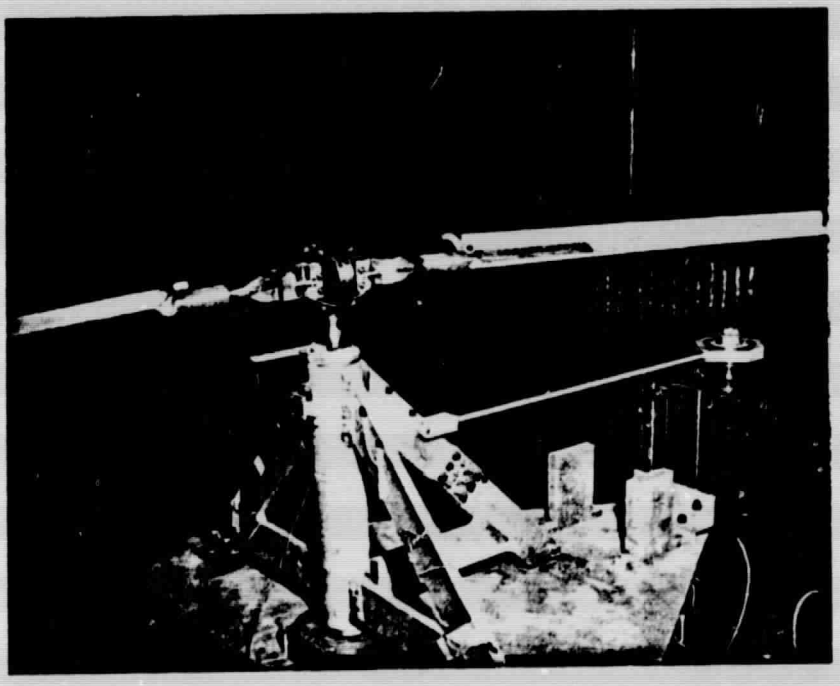

Close-up of Hub and Mechanical Shaker

Figure 1. Photograph of Thrust Stand and Rotor System

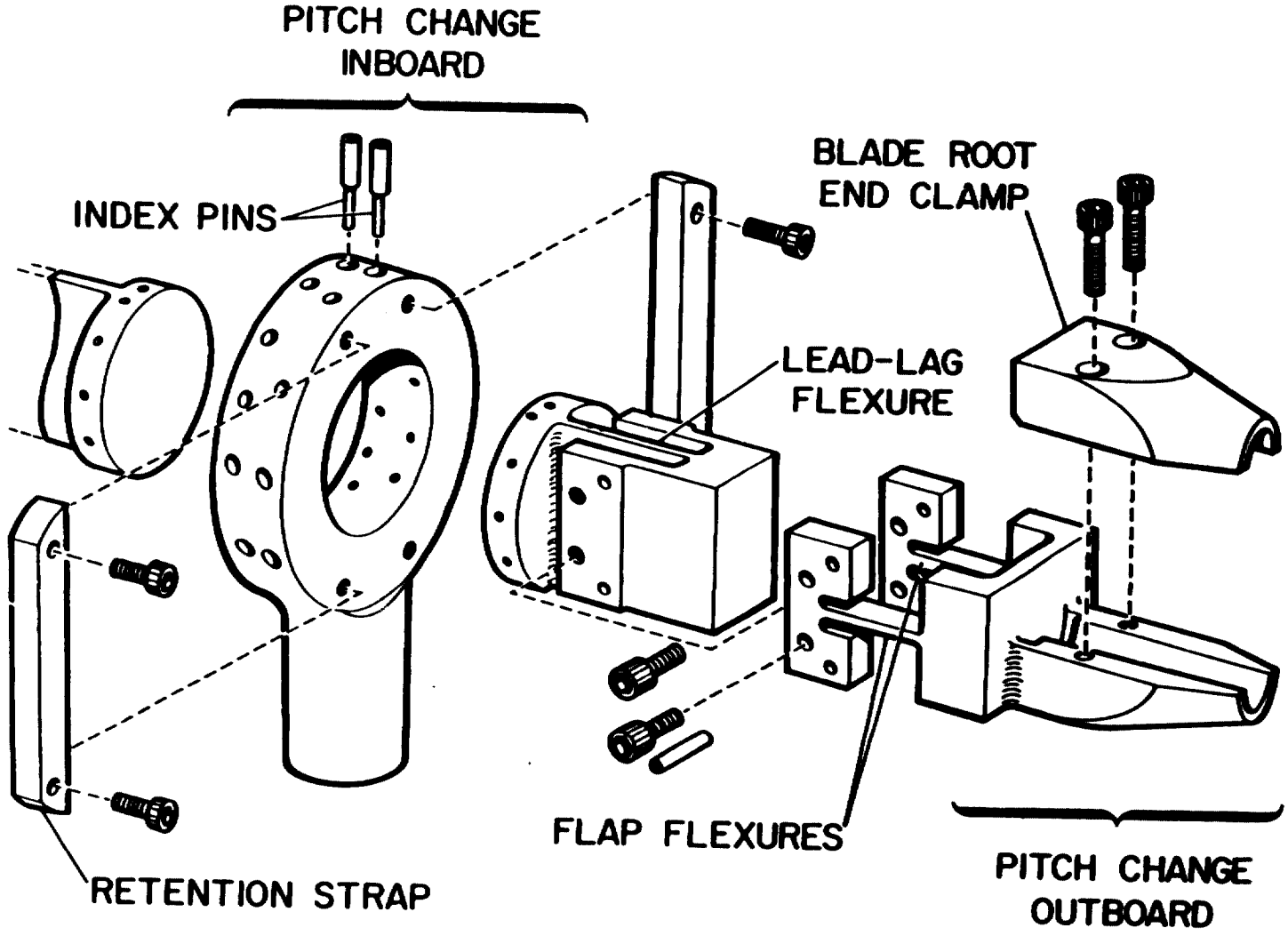

Figure 2. Exploded View of Flexure Hub.

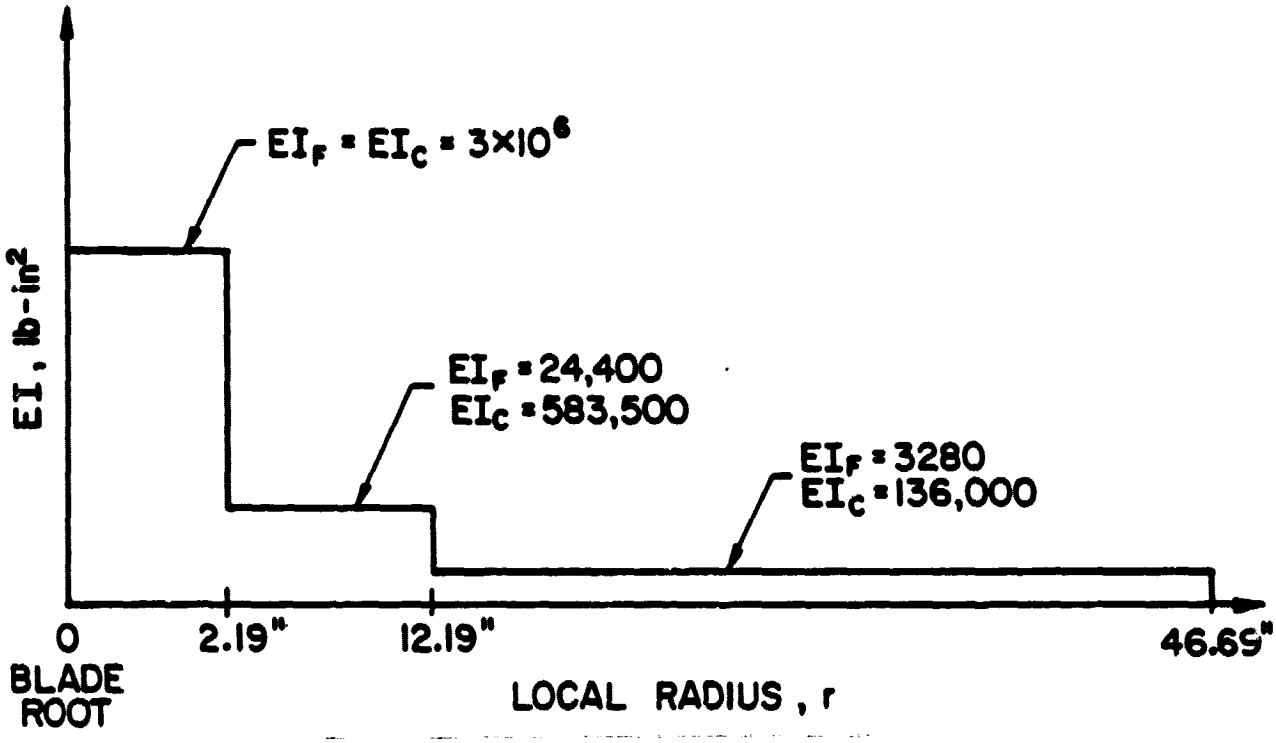

a.) Stiffness Distribution.

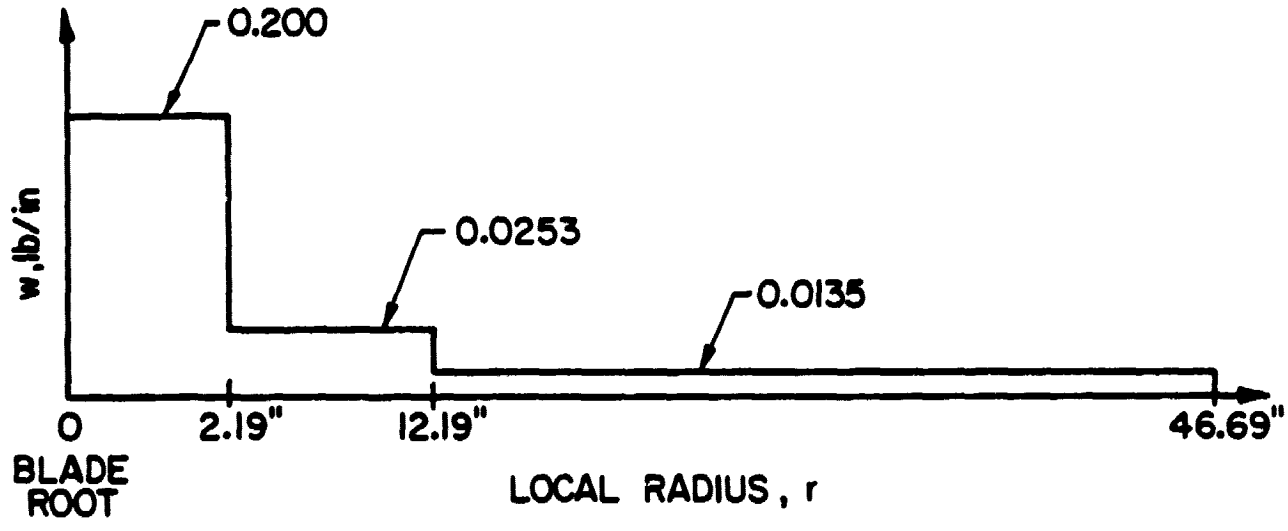

b.) Weight Distribution.

Figure 3. Stiffness and Weight Distribution of Rotor Blade.

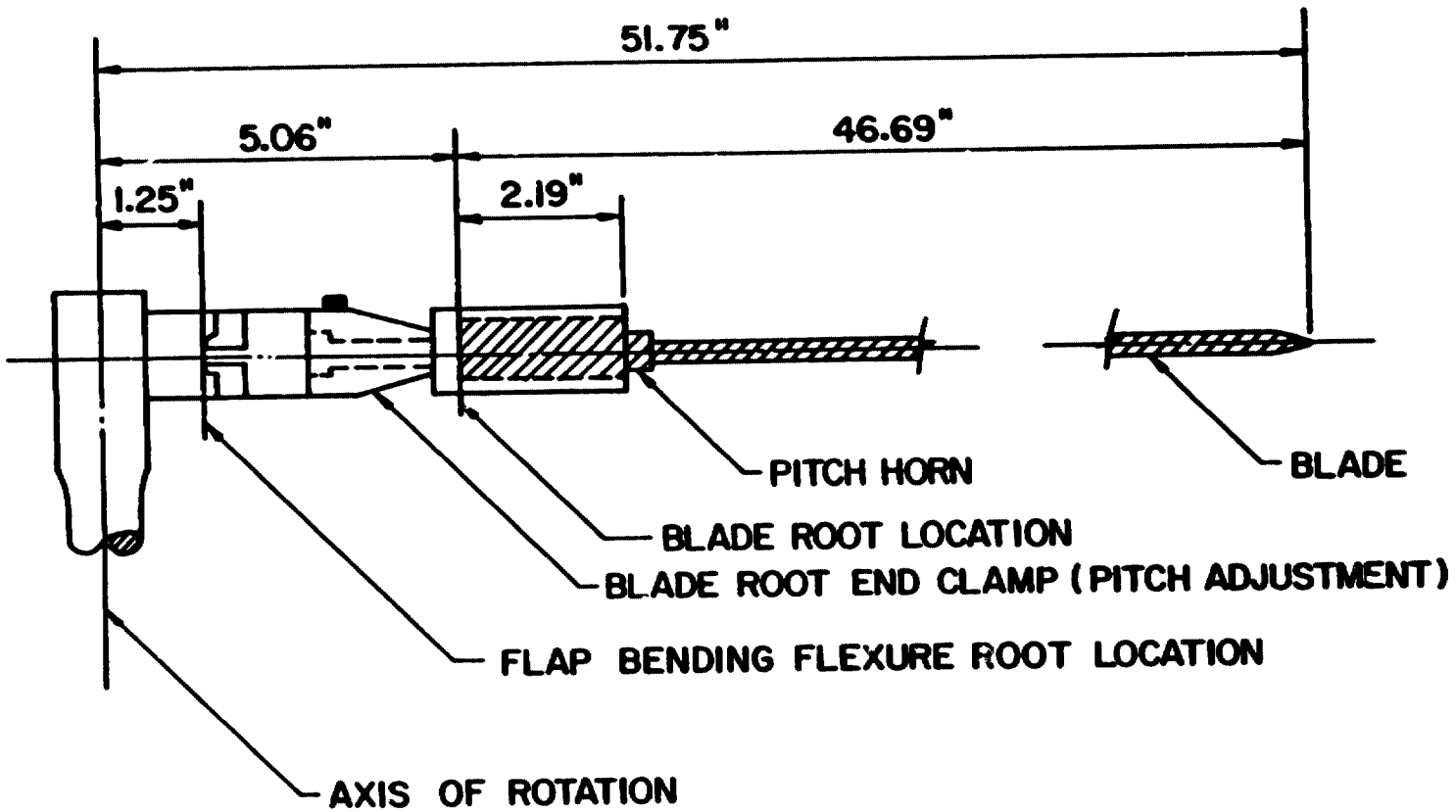

Figure 4. Geometry of Hub and Blade. Blade Shown Cross-Hatched.

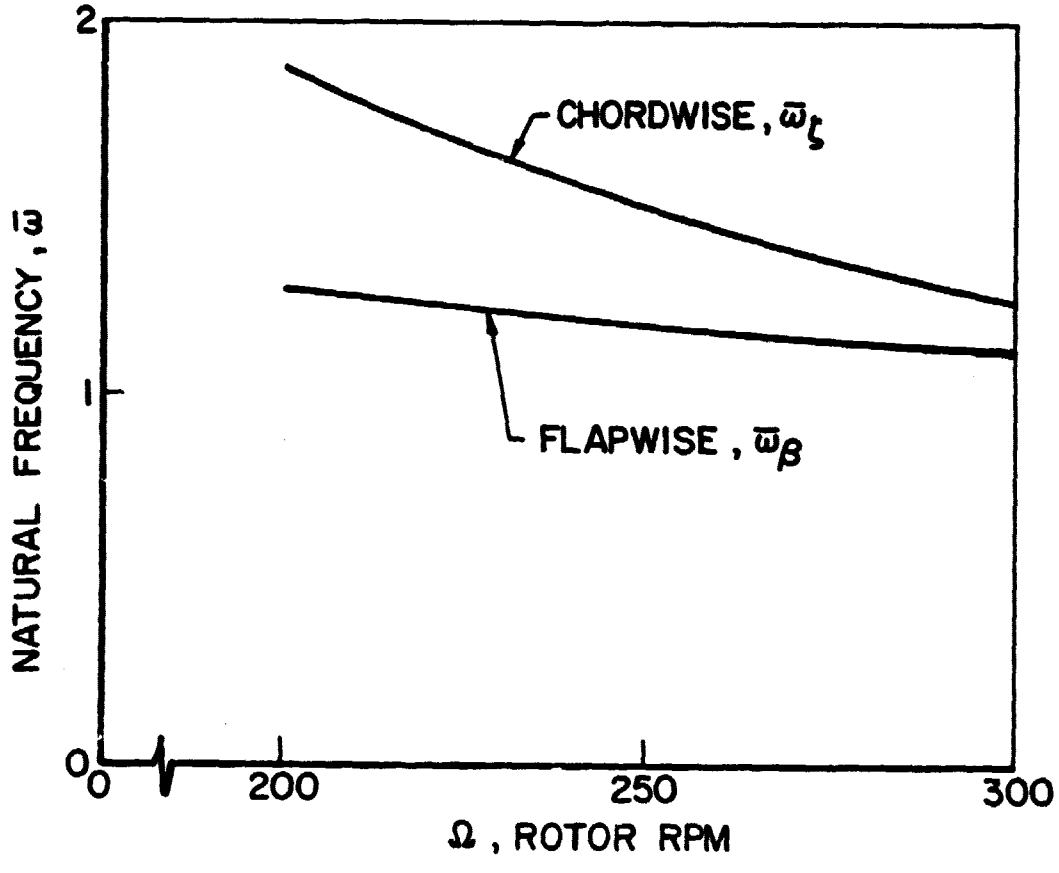

$\theta_s = 0$

$K_F = 1$

$K_C = 0$

Figure 5. Calculated Rotor Flapwise and Chordwise Natural Frequencies as a Function of Rotor RPM.

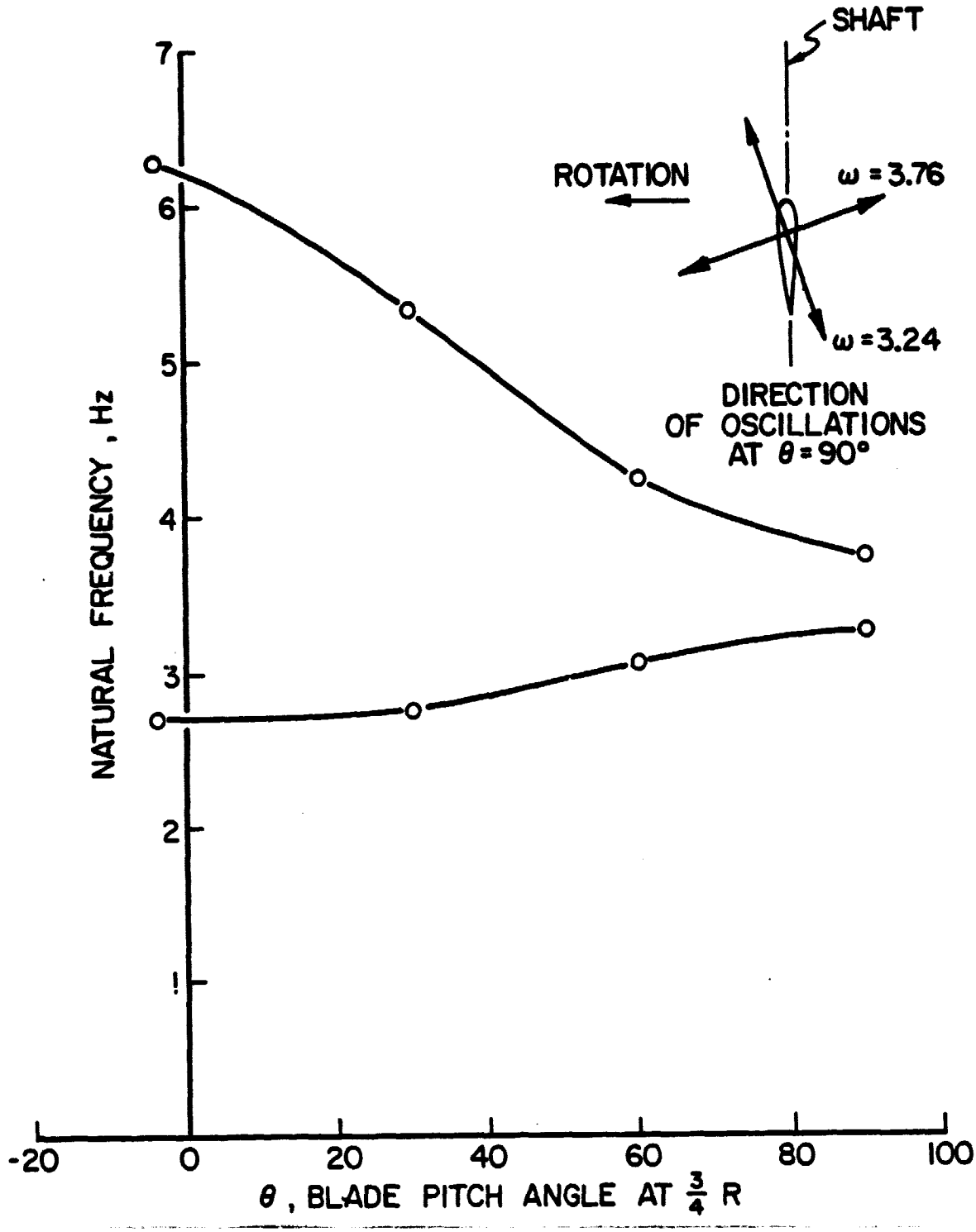

Figure 6. Experimentally Determined Non-Rotating Natural Frequencies of Rotor as a Function of Blade Pitch Angle.

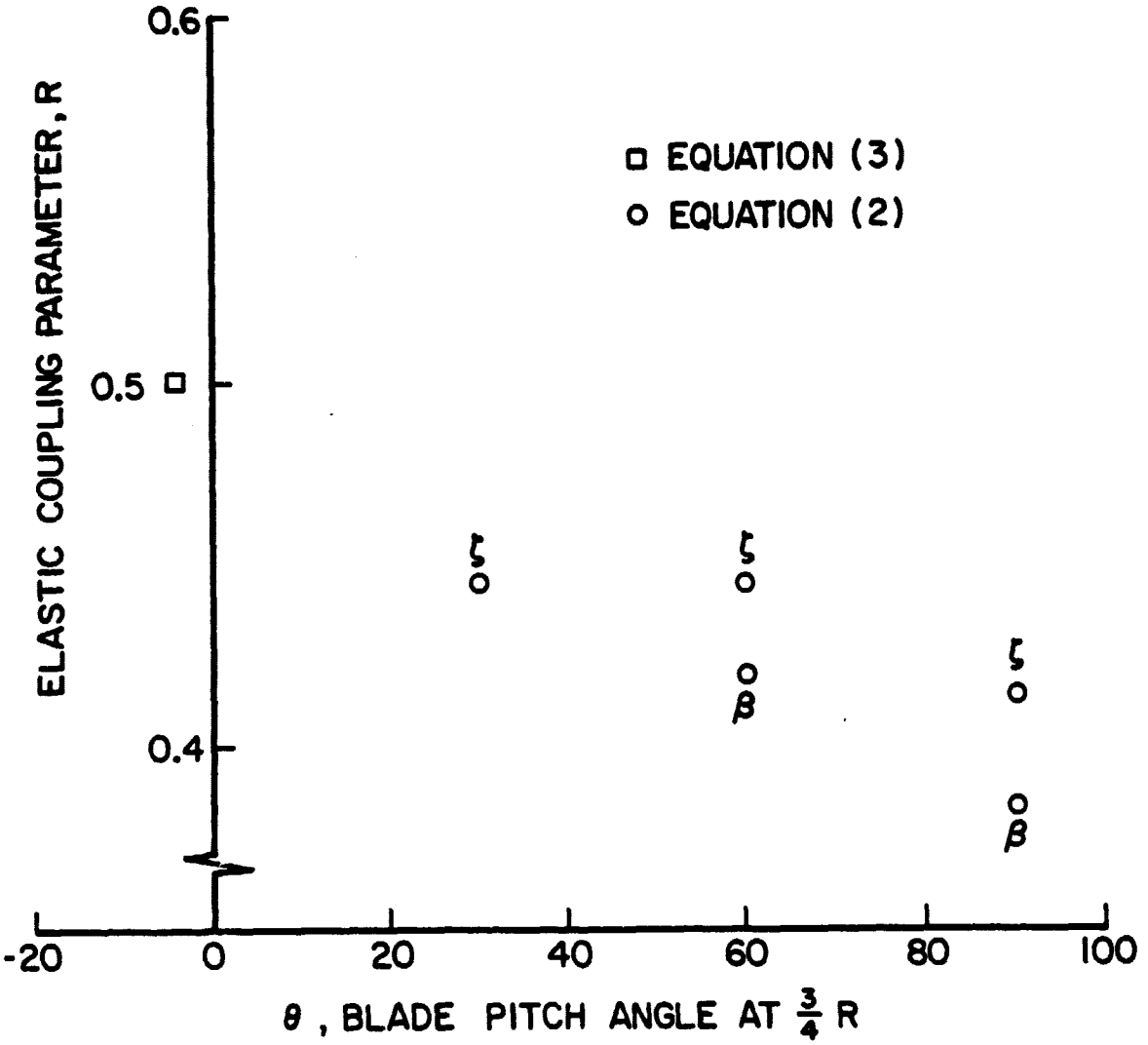

Figure 7. Calculated Values of the Elastic Coupling Parameter R as a Function of Blade Pitch Angle.

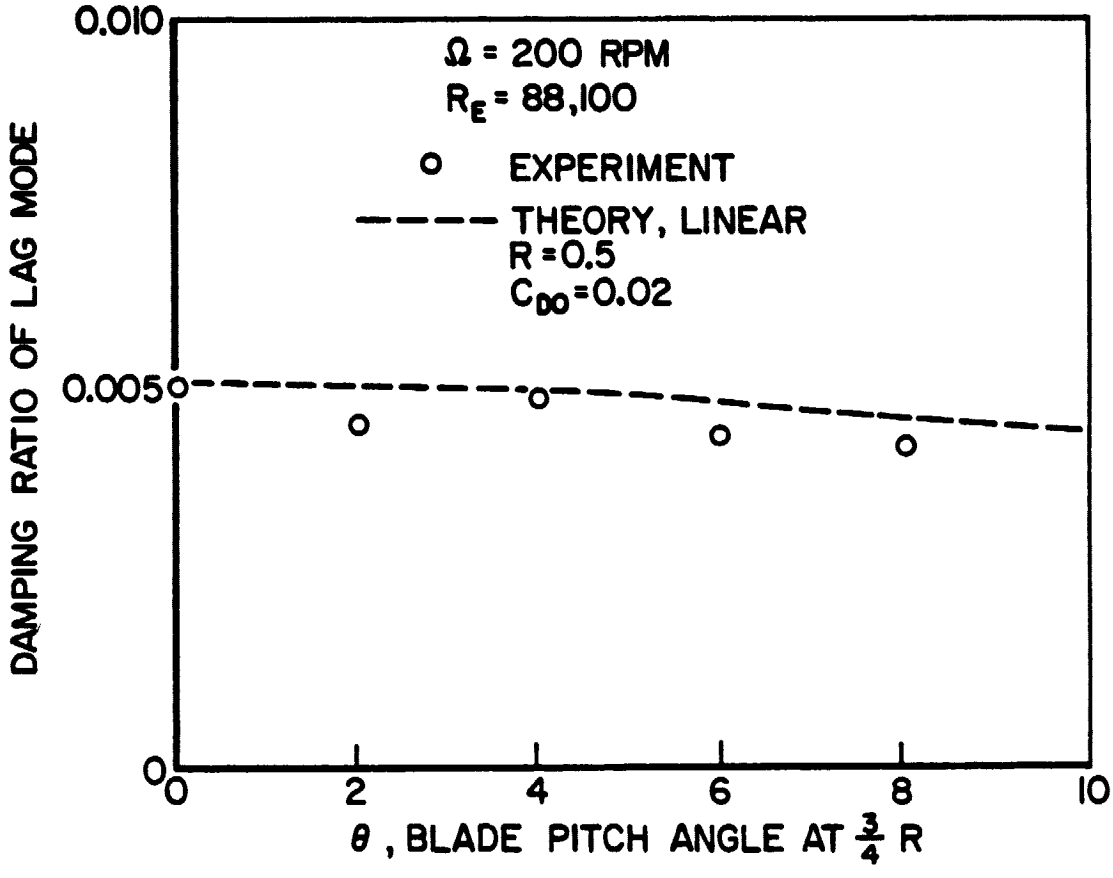

Figure 8. Comparison of Experiment and Theory for Damping Ratio of Lag Mode at Ω = 200 RPM.

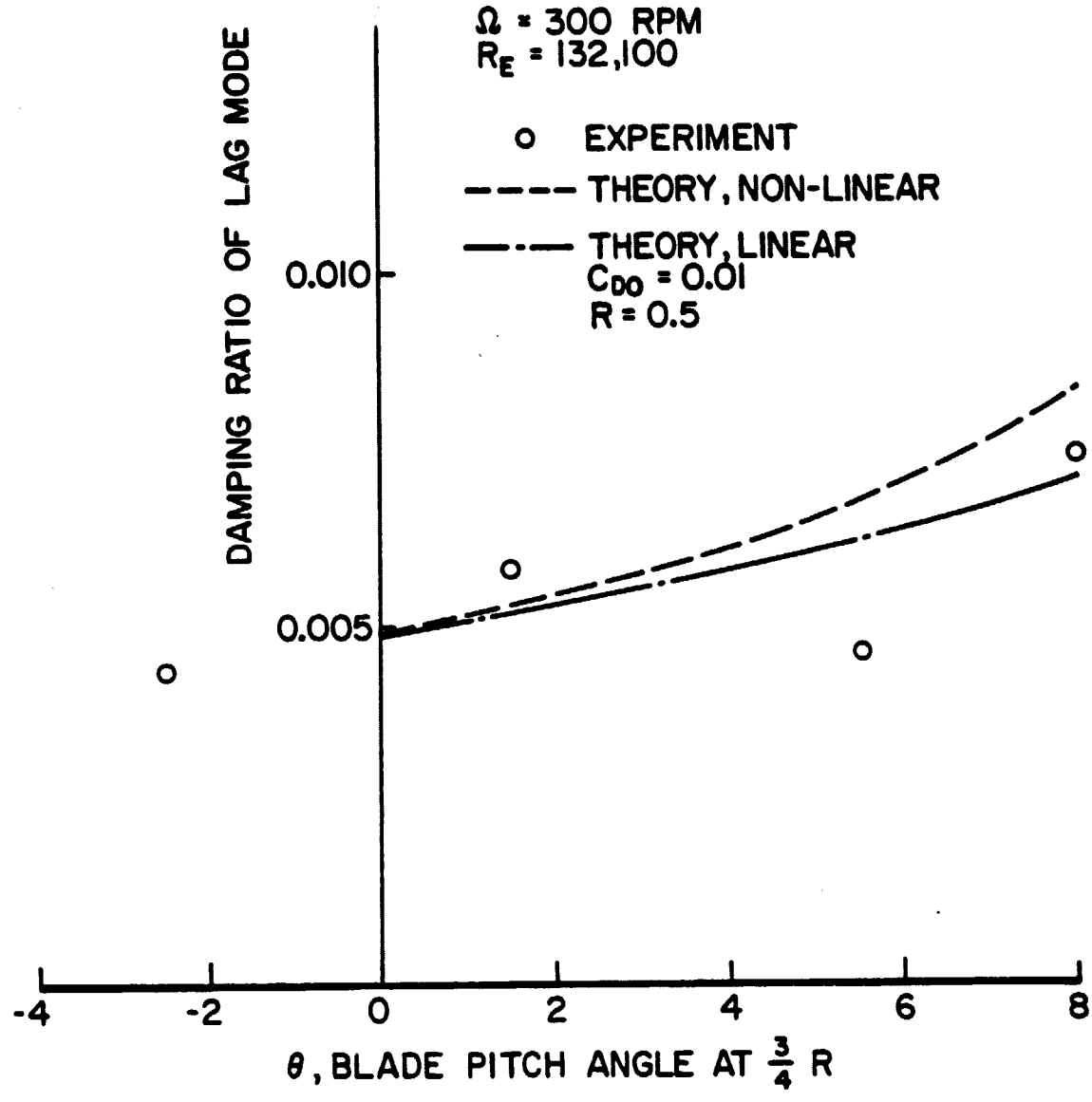

Figure 9. Comparison of Experiment and Theory for Damping Ratio of Lag Mode at Ω = 300 RPM.

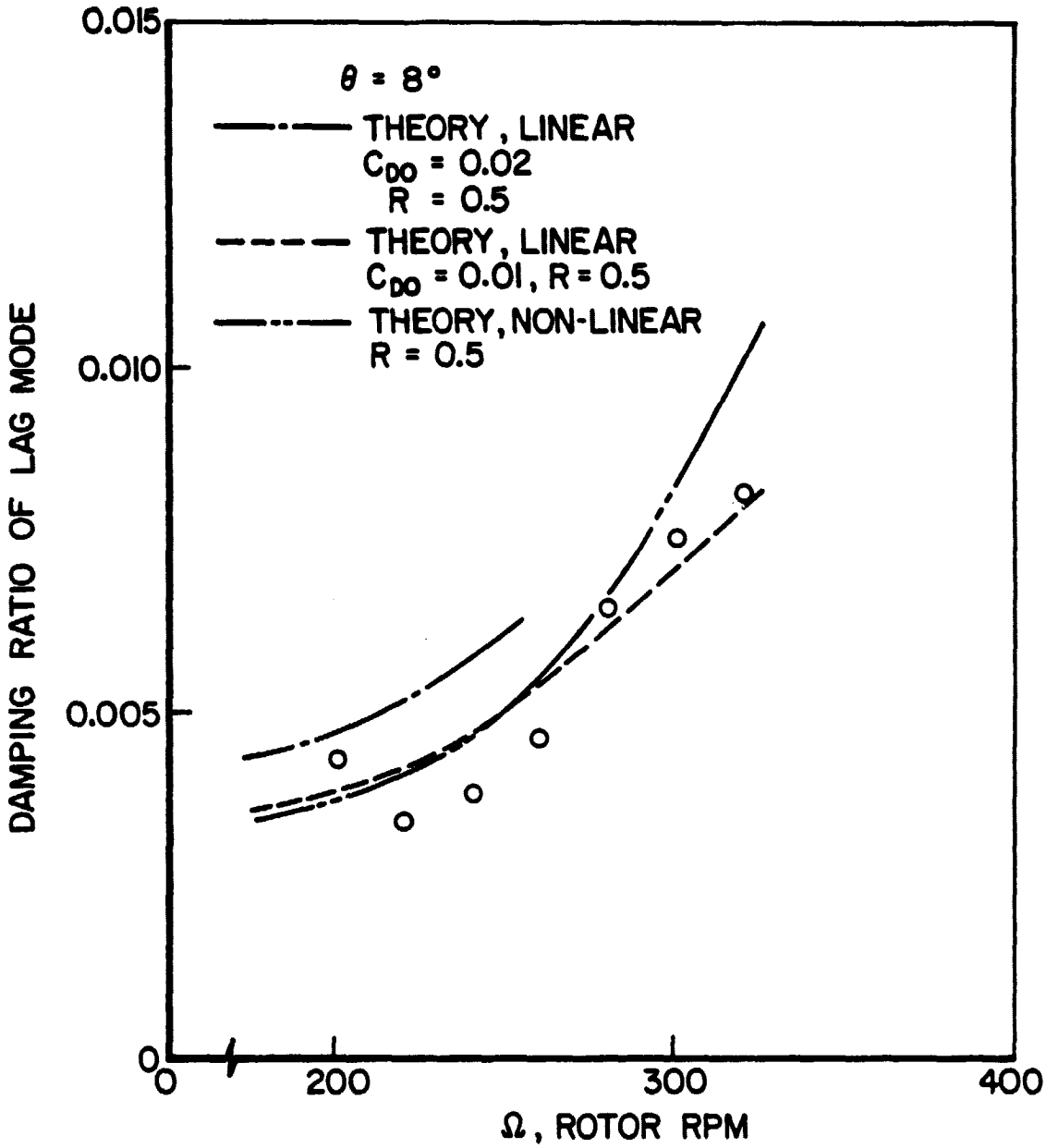

Figure 10. Comparison of Experiment and Theory for Damping Ratio of Lag Mode as a Function of Rotor RPM for $\theta = 8^{\circ}$.

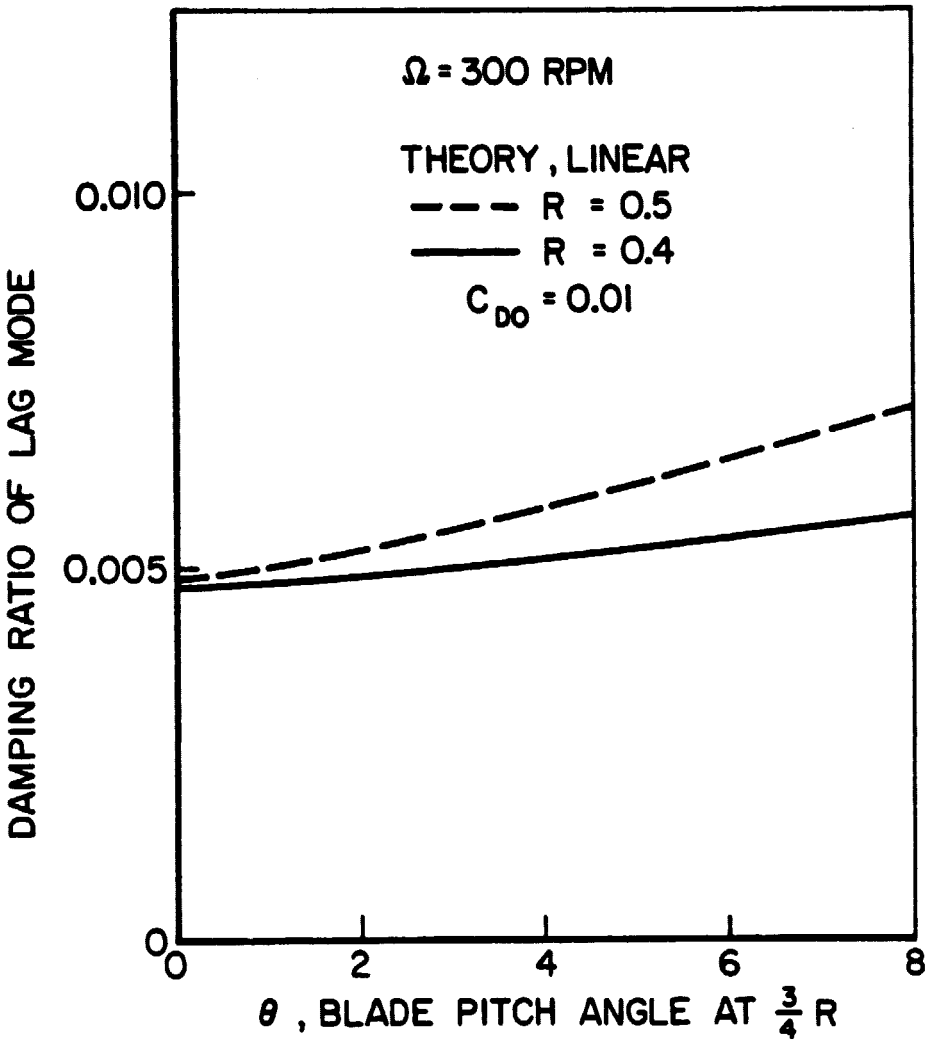

Figure 11. Influence of R on Damping Ratio of Lag Mode.